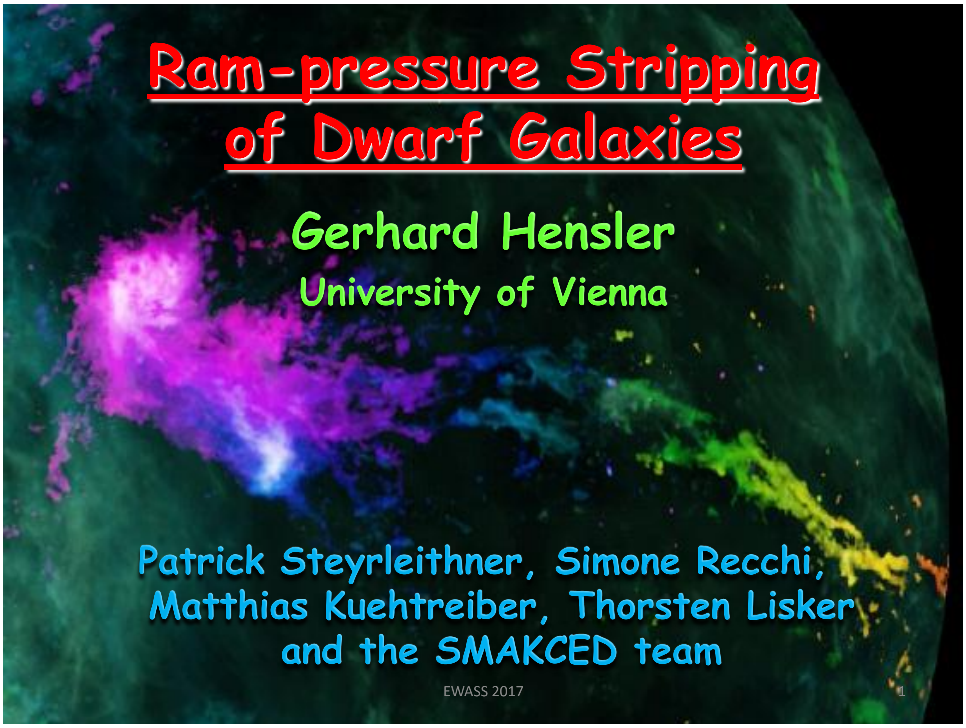
Ram-pressure Stripping
of Dwarf Galaxies
Gerhard Hensler
University of Vienna
Patrick Steyrleithner, Simone Recchi,
Matthias Kuehtreiber, Thorsten Lisker
and the SMAKCED team
EWASS 2017
1

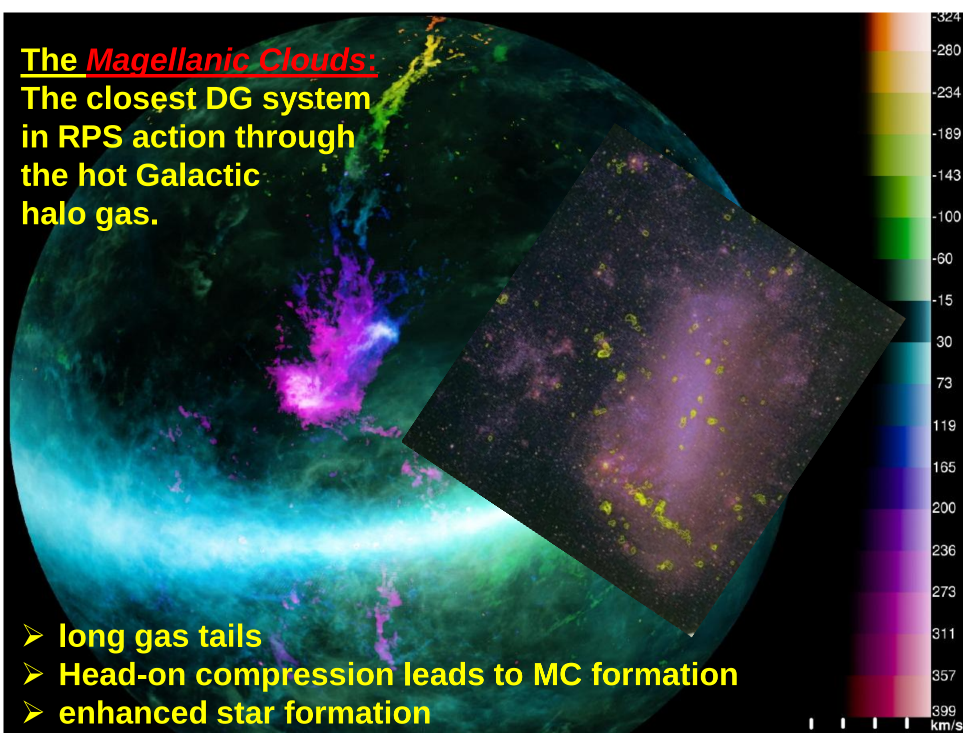
The Magellanic Clouds:
The closest DG system
in RPS action through
the hot Galactic
halo gas.
➢ long gas tails
➢ Head-on compression leads to MC formation
➢ enhanced star formation
-324
-280
-234
-189
-143
-100
-60
-15
30
73
119
165
200
236
273
311
357
399
km/s

Ram-pressure Stripping of Spirals

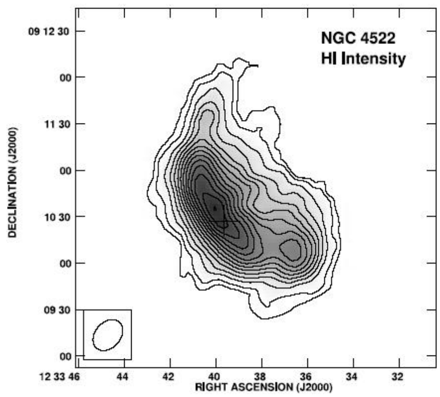

FIG. 2.—H I total intensity (moment 0) map. The cross marks H I kinematic center. Note peak in projected H I surface density to the northeast of nucleus, and the H I asymmetry in the disk. The lowest contour is 25 mJy beam^{-1} km s^{-1}, which corresponds to 0.6 $M_{\odot}$ pc^{-2} = 8×10^{19} cm^{-2}. The contour increments are 0.8, 1.6, 3.2, 4.8, 6.4, 8.0, 9.6, 11.2, 12.8, 14.4, 16.0, 17.6, 19.2, and 20.8×10^{20} cm^{-2}.

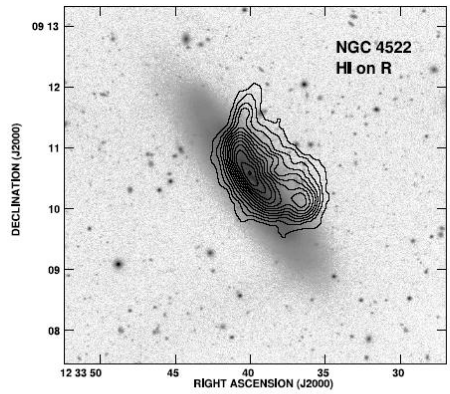

FIG. 3.—H I moment 0 contour map of NGC 4522 on *R*-band gray-scale image from the WIYN telescope from Kenney & Koopmann (1999). The lowest H I contour level and contour increments are 50 mJy beam^{-1} km s^{-1}. The optical image is shown with logarithmic stretch. Note the undisturbed outer stellar disk.

NGC 4522 reveals a truncated HI disk and its bent-up.

NGC 4522 moves with ~1300 km/s relatively to the Virgo IGM. Gas is stripped off towards one direction.

THE ASTROPHYSICAL JOURNAL, 176:1–19, 1972 August 15

ON THE INFALL OF MATTER INTO CLUSTERS OF GALAXIES AND SOME EFFECTS ON THEIR EVOLUTION*

JAMES E. GUNN
Hale Observatories, California Institute of Technology, Carnegie Institution of Washington
AND
J. RICHARD GOTT III
Princeton University Observatory
Received 1972 January 24

ABSTRACT

A theory of infall of material into clusters of galaxies is developed and applied to the Coma cluster. It is suggested that the infall phenomenon is responsible for the growth of cluster galaxies. The generation of a hot intracluster medium is discussed and its relation to the observed absence of normal spirals in rich clusters investigated. The inference made earlier by Gott and Gunn that the observed X-ray luminosity of Coma puts severe constraints on the deceleration parameter q_0 is further elucidated. We discuss the relation of these phenomena to the morphology of clusters, and find that some observed regularities in their observed properties can be explained.

however, some interesting effects *if there is any gas left*. We here discuss briefly some of these.

Consider first a cluster with a hot, smooth (the distribution *must* clearly be smooth if the temperature is high) intracluster medium, and a galaxy moving through that medium. The interstellar material in the galaxy feels the ram pressure of the intracluster medium as it flows past. This ram pressure is

$$P_r \approx \rho_e v^2 , \qquad (61)$$

where ρ_e is the external (to the galaxy, i.e., the intracluster) density, and v the velocity of the galaxy. If the galaxy is a typical spiral, this material will be held in the plane by a force per unit area which cannot exceed

$$\mathfrak{F} = 2\pi G \sigma_s \sigma_g , \qquad (62)$$

where σ_s is the star surface density and σ_g the gas surface density on the disk of the galaxy. For a typical large spiral with a mass of $10^{11} M_\odot$ and a radius of 10 kpc, $\sigma_s \sim 0.06$ g cm^{-2}; a gas layer 200 pc thick with a density of one atom per cm^3 has a surface density of 10^{-3} g cm^{-2}, corresponding to a restoring force of about 2.5×10^{-11} dyn cm^{-2}. The ram pressure, from equation (61), is, for a galaxy moving at the rms velocity of 1700 km s^{-1}, $5 \times 10^{-8} n$ dyn cm^{-2}; where n is the intracluster number density. *Thus if the intracluster density exceeds 5×10^{-4} atoms cm^{-3}, then a typical galaxy moving in it will be stripped of its interstellar material.* The central density corresponding to the distribution (60) has $n = 0.16$, so if as little as 3×10^{-3} of the mass of the cluster is in gas, a galaxy moving through the central regions will be stripped. We will see below that the X-ray data indicate that the *present* gas density comprises roughly 3 percent of the cluster mass, so we expect *no normal spirals* in the central regions of clusters like Coma. The lack of such systems is, of course, observed, and it was originally suggested (Baade

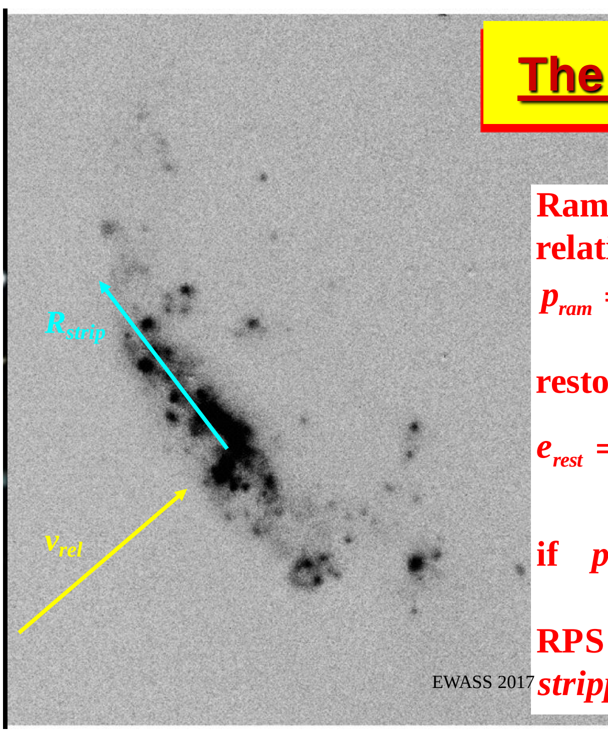

The effect of RPS

Ram Pressure by the relative motion of the IGM :

$$p_{ram} = \rho_{IGM} \cdot v_{rel}^2$$

restoring energy density :

$$e_{rest} = \frac{d\Phi}{dz}(r) \cdot \Sigma_{ISM}(r)$$

if $p_{ram} > e_{rest}$

RPS works until the *stripping radius R_{strip}*

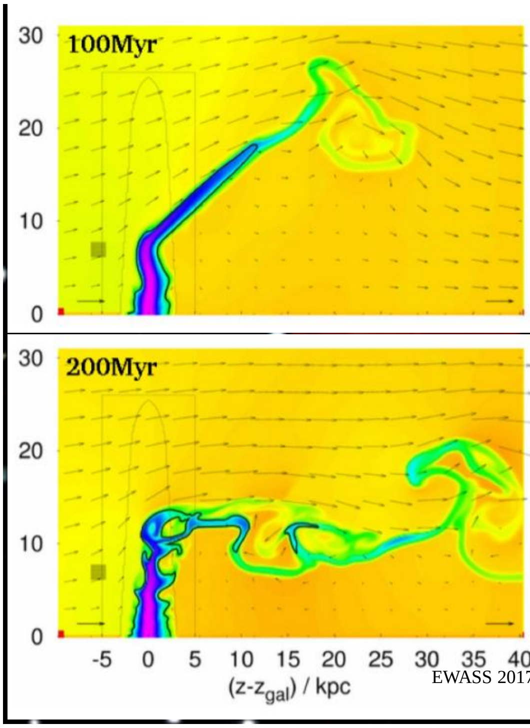

Model parameters:

T_{ICM}	$= 5\times10^7$K
Ma	= 0.7
n_{ICM}	$= 10^{-3}$ cm^{-3}
M_{ISM}	$= 10^9 M_\odot$
M_{disk}	$= 10^{10} M_\odot$

The mass loss by means of stripping is characterized by 2 stripping stages:

1. The ram pressure bends the disk backwards ⇒ immediate and massive stripping;
2. Kelvin-Helmholtz instability caused by the sheering motion of the stream at the disk's edges grazes the gas off.

Roediger & Hensler (2005) A&A, 433

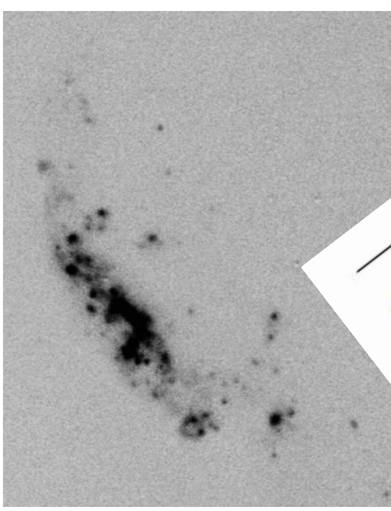

Kenney & Koopman (1999), AJ, 117

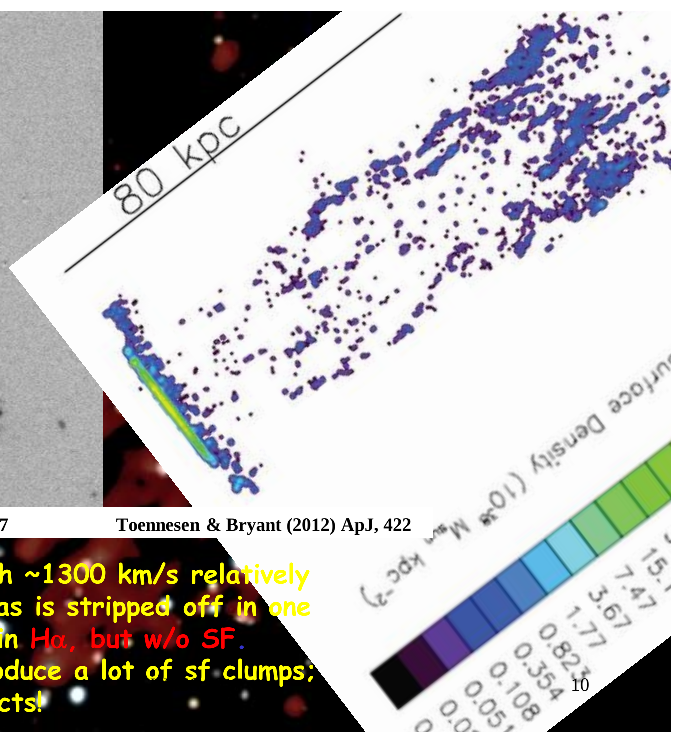

Toennesen & Bryant (2012) ApJ, 422

NGC 4522 moves with ~1300 km/s relatively to the Virgo IGM. Gas is stripped off in one direction and shines in Hα, but w/o SF.
Numerical models produce a lot of sf clumps;
Yet numerical artefacts!

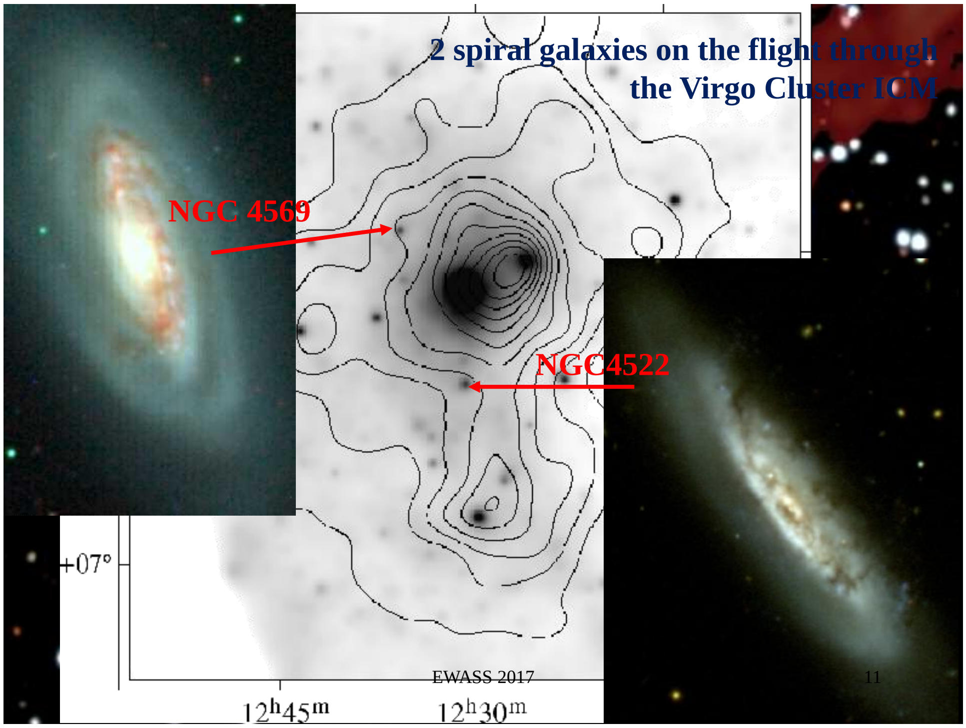
2 spiral galaxies on the flight through
the Virgo Cluster ICM
NGC 4569
NGC4522
+07°
12h45m
12h30m
EWASS 2017
11

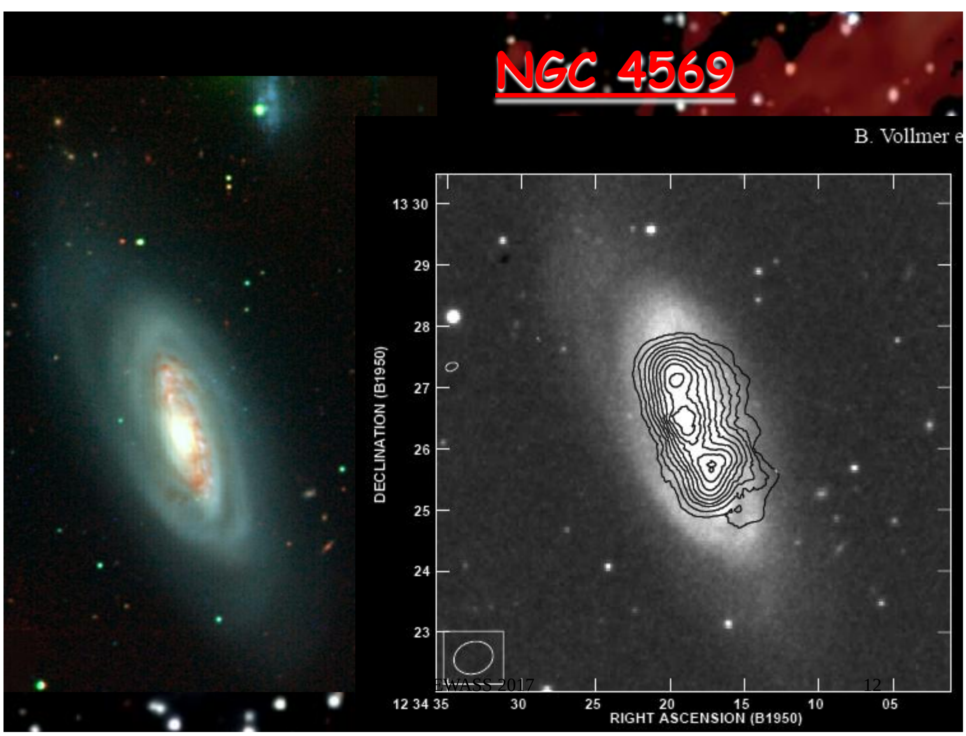
NGC 4569
B. Vollmer e
13 30
29
28
27
26
25
24
23
DECLINATION (B1950)
12 34 35
30
25
20
15
10
05
RIGHT ASCENSION (B1950)
EWASS 2017
12

NGC 4569 is HI deficient and shows an Hα filament towards the W.

A bipolare X-ray outflow is asymmetric: compressed to the E, also extended to the W.

Tschöke, G.H., Junkes 2001, A&A, 380

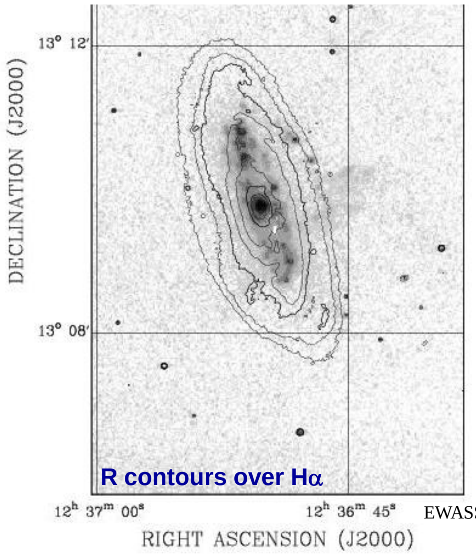

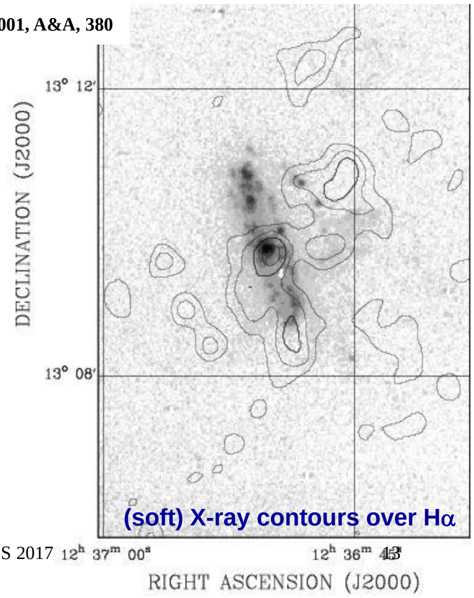

EWASS 2017

Boselli et al. (G.H.), 2016, A&A, 587

Sensitive deep Hα imaging uncovers long Hα tails without star formation:
Hα is a necessary, but not sufficient condition!
Excitation by hot IGM!

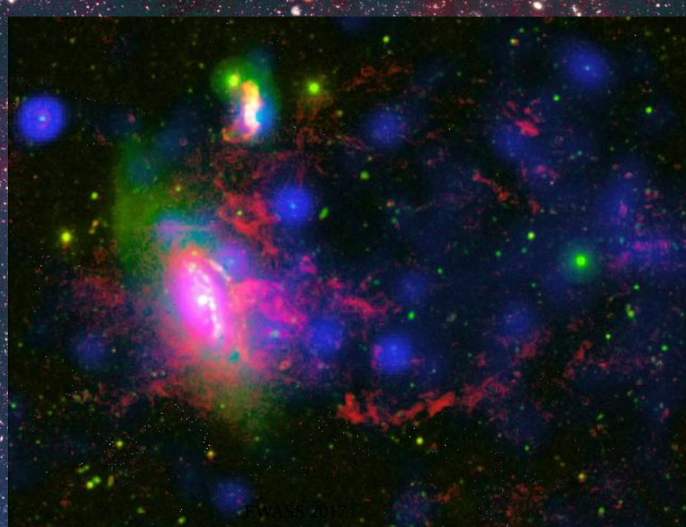

EWASS 2017

dE dominate in clusters

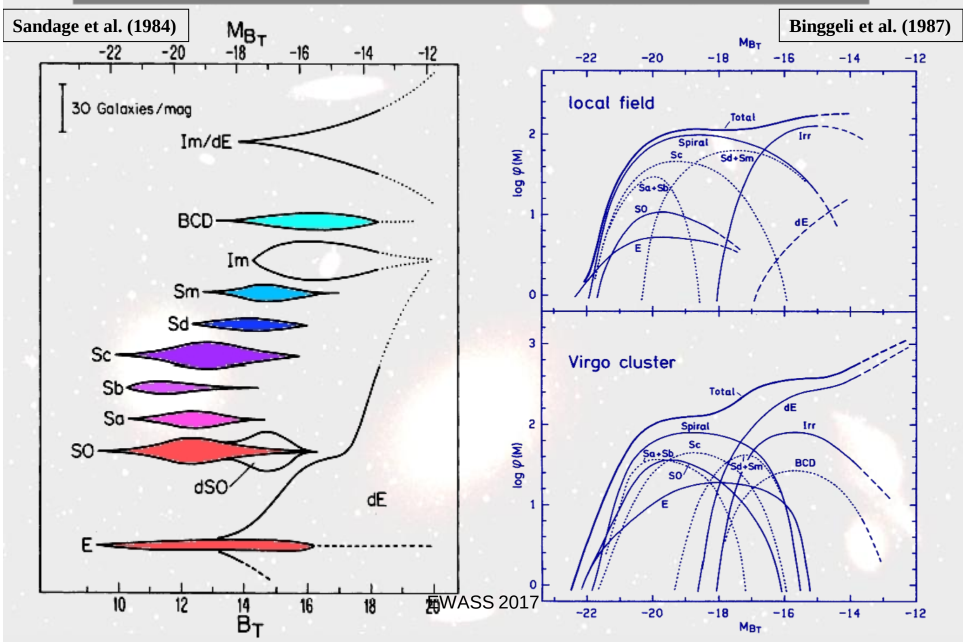

- The fractional density of dIrrs in clusters is a bit less than in the field.
- dEs dominate the morphology in clusters!
- How many dEs originally in cluster?

What makes dIrrs → dEs?

- Which process drives gas loss?

1. Galactic winds, gas expulsion
2. Tidal stripping
3. Ram-pressure stripping

Correlations of different galaxy types

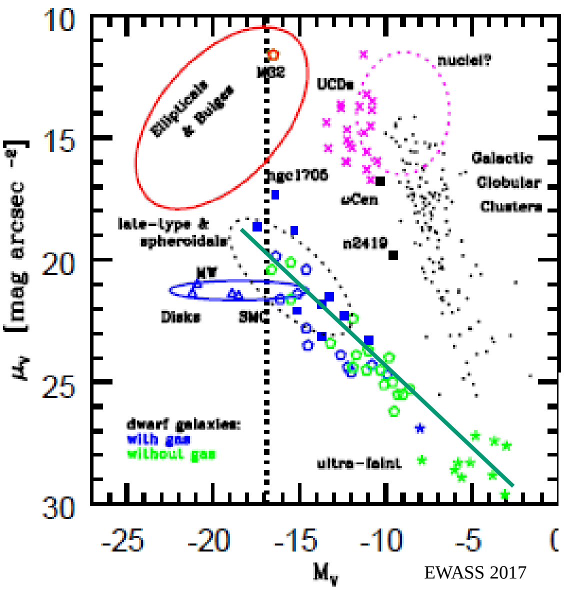

Tolstoy et al. (2010) ARAA, 47

All "normal" DGs, dEs and dIrrs, follow the same relations even to their faintest end, but differ from UCDs+GCs and from the Hubble-type galaxies.

Are morphological transformations possible and how?

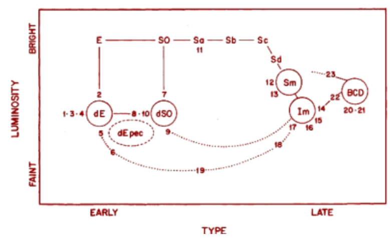

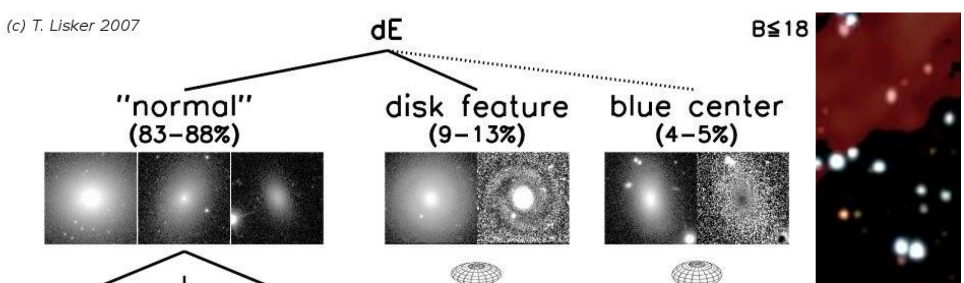

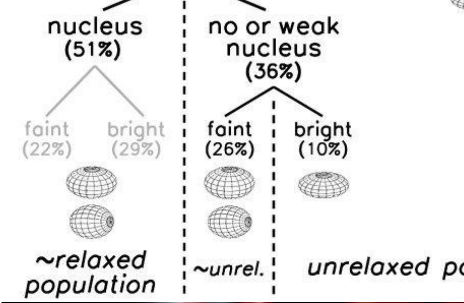

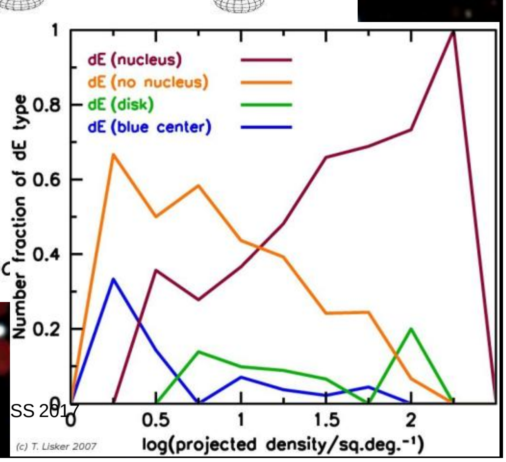

dEs in Virgo show a variety of shapes + properties that seem to correlate with the radial cluster distribution.

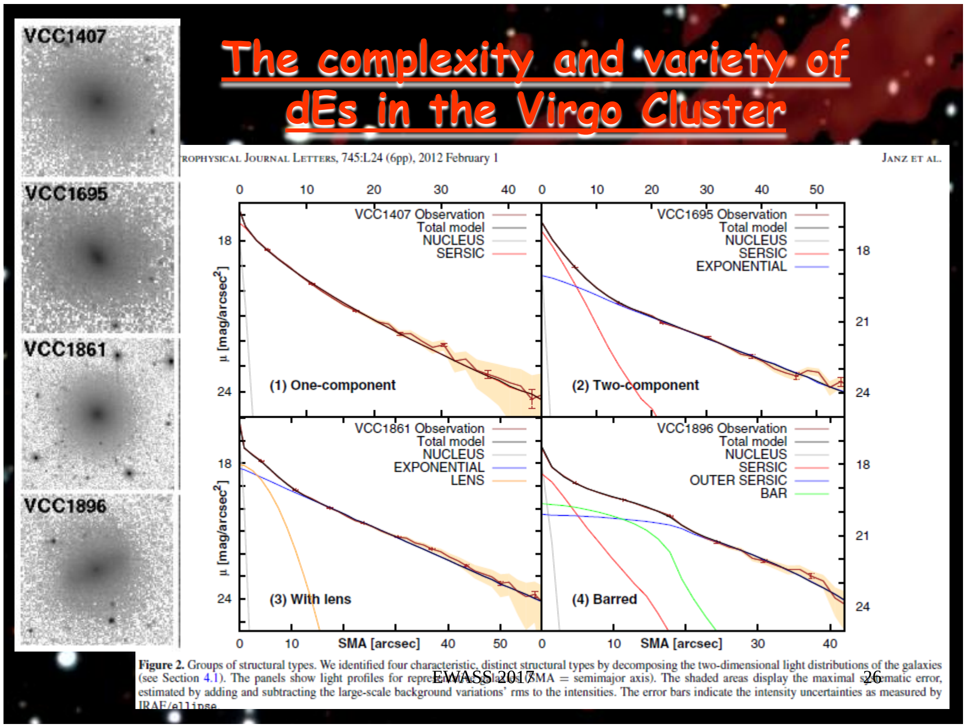
The complexity and variety of dEs in the Virgo Cluster
VCC1407
VCC1695
VCC1861
VCC1896
The Astrophysical Journal Letters, 745:L24 (6pp), 2012 February 1
Janz et al.
VCC1407 Observation
Total model
NUCLEUS
SERSIC
(1) One-component
VCC1695 Observation
Total model
NUCLEUS
SERSIC
EXPONENTIAL
(2) Two-component
VCC1861 Observation
Total model
NUCLEUS
EXPONENTIAL
LENS
(3) With lens
VCC1896 Observation
Total model
NUCLEUS
SERSIC
OUTER SERSIC
BAR
(4) Barred
μ [mag/arcsec²]
SMA [arcsec]
Figure 2. Groups of structural types. We identified four characteristic, distinct structural types by decomposing the two-dimensional light distributions of the galaxies (see Section 4.1). The panels show light profiles for representative examples (SMA = semimajor axis). The shaded areas display the maximal systematic error, estimated by adding and subtracting the large-scale background variations' rms to the intensities. The error bars indicate the intensity uncertainties as measured by IRAF/ellipse.
EWASS 2017
26

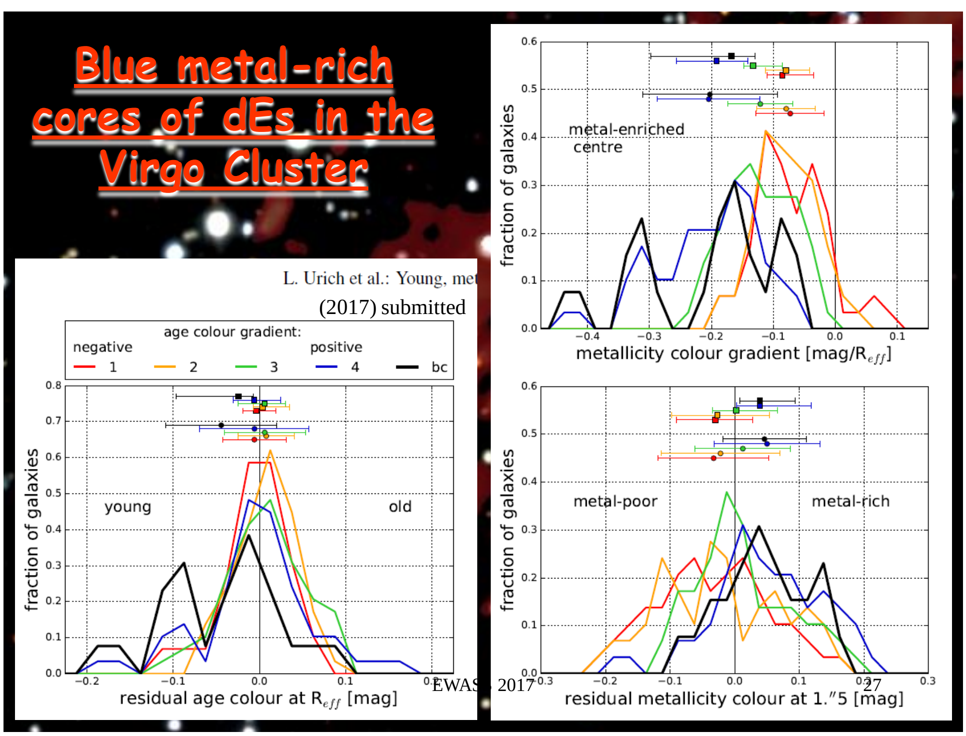
Blue metal-rich cores of dEs in the Virgo Cluster
L. Urich et al.: Young, met
(2017) submitted
age colour gradient:
negative
positive
1
2
3
4
bc
young
old
fraction of galaxies
residual age colour at R_{eff} [mag]
metal-enriched centre
metallicity colour gradient [mag/R_{eff}]
metal-poor
metal-rich
residual metallicity colour at 1.″5 [mag]
EWASS 2017
27

Star-formation history in Fornax dEs

Koleva et al. 2009, MNRAS, 396

Star formation histories in dEs

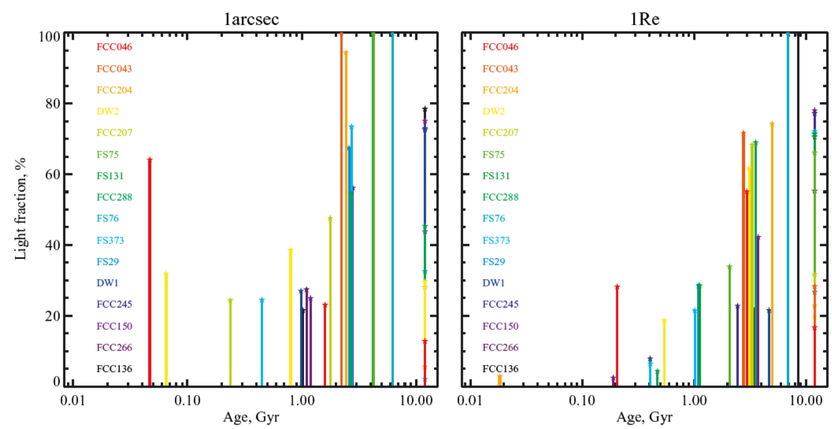

Light fractions of each burst for all the galaxies. Each galaxy is represented with a different colour indicated in the frame. Each star form
s a vertical bar whose position is its age and height its light contribution to the total spectrum.

EWASS 2017

Dwarf Ell. in Clusters show

- ✓Multi stellar components:
  Young metal-rich centers
- ✓Blue cores
- ✓Gas in the centers
- ✓Central Hα emission

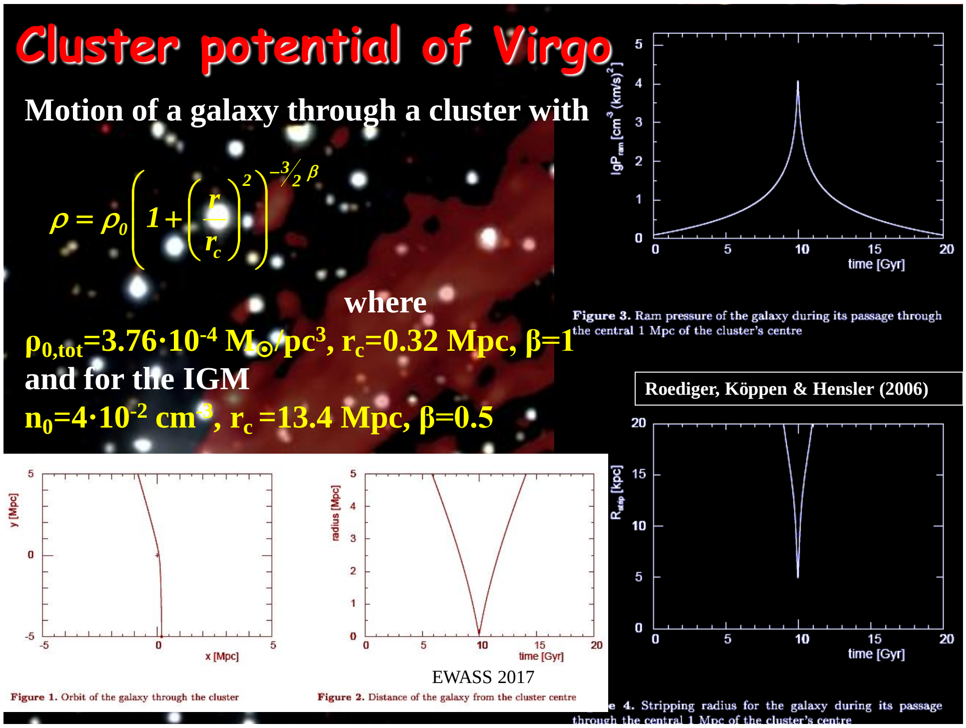
Cluster potential of Virgo
Motion of a galaxy through a cluster with
$\rho = \rho_0 \left(1 + \left(\frac{r}{r_c}\right)^2\right)^{-3/2\,\beta}$
where
$\rho_{0,tot}$=3.76·10^{-4} $M_\odot$/pc^3, r_c=0.32 Mpc, β=1
and for the IGM
n_0=4·10^{-2} cm^{-3}, r_c =13.4 Mpc, β=0.5
time [Gyr]
Figure 3. Ram pressure of the galaxy during its passage through the central 1 Mpc of the cluster's centre
Roediger, Köppen & Hensler (2006)
y [Mpc]
x [Mpc]
radius [Mpc]
time [Gyr]
EWASS 2017
Figure 1. Orbit of the galaxy through the cluster
Figure 2. Distance of the galaxy from the cluster centre
time [Gyr]
e 4. Stripping radius for the galaxy during its passage through the central 1 Mpc of the cluster's centre

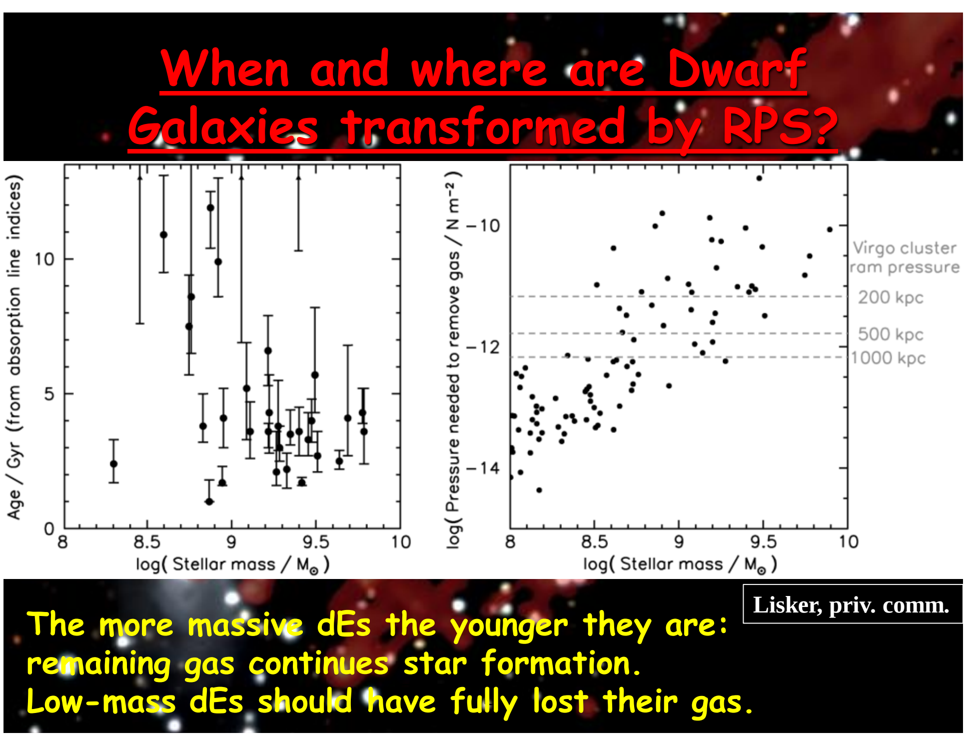
When and where are Dwarf Galaxies transformed by RPS?
Age / Gyr (from absorption line indices)
log(Stellar mass / $M_\odot$)
log(Pressure needed to remove gas / N m^{-2})
log(Stellar mass / $M_\odot$)
Virgo cluster ram pressure
200 kpc
500 kpc
1000 kpc
Lisker, priv. comm.
The more massive dEs the younger they are: remaining gas continues star formation.
Low-mass dEs should have fully lost their gas.

Gas Loss of DGs by RPS

Mori & Burkert (2000)

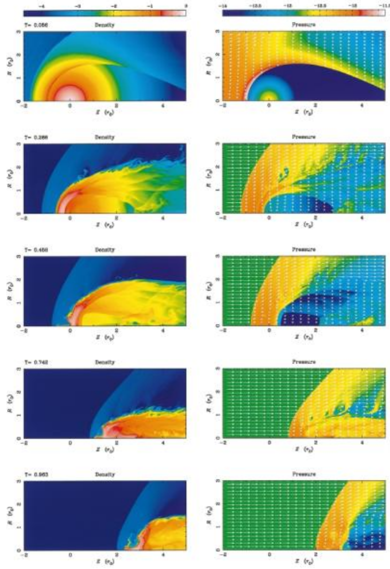

FIG. 2.—Snapshots for the model with core mass $M_c = 10^7\ M_\odot$, number density of the ICM $n_{CG} = 10^{-4}\ cm^{-3}$, and relative velocity of the galaxy $v_{gal} = 1000\ km\ s^{-1}$ as a function of elapsed time at 5.61×10^6, 2.86×10^7, 4.58×10^7, 7.42×10^7, and 9.63×10^7 yr. The left and the right color images show the logarithmic density distribution and the logarithmic pressure distribution, respectively. Arrows in the right panels indicate the velocity vector of the gas flow at each point.

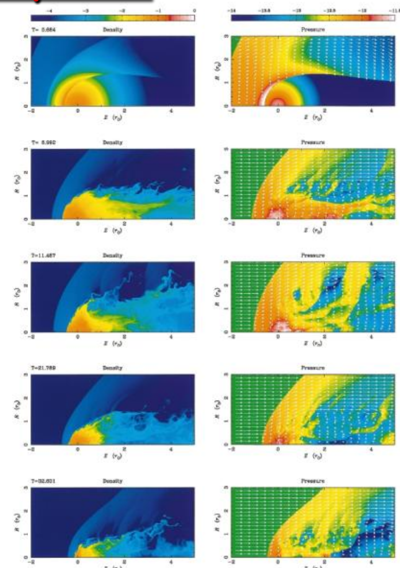

FIG. 3.—Snapshots for the model with core mass $M_c = 10^{10}\ M_\odot$, number density of the ICM $n_{CG} = 10^{-4}\ cm^{-3}$, and relative velocity $v_{gal} = 1000\ km\ s^{-1}$ as a function of elapsed time at 6.84×10^7, 6.99×10^8, 1.15×10^9, 2.18×10^9, and 3.26×10^9 yr. The left and the right color images show the logarithmic density distribution and the logarithmic pressure distribution, respectively. Arrows in the right panels indicate the velocity vector of the gas flow at each point.

EWASS 2017 32

see also: Roediger & Hensler (2005)

Noeske et al. (2000) A&A, 361, 33

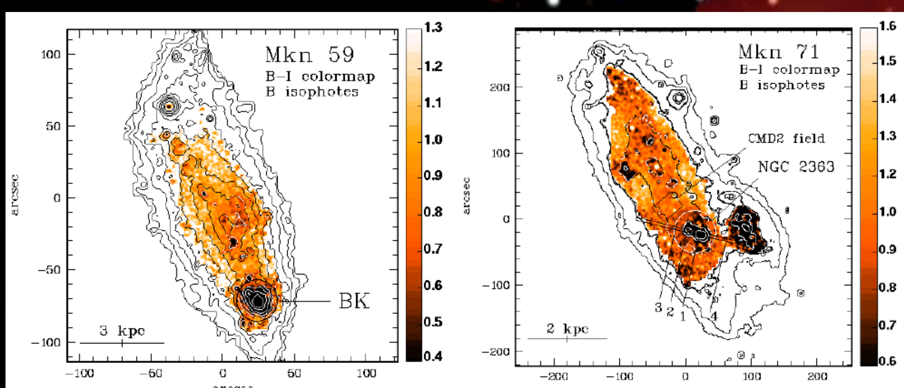

Fig. 1. $(B - I)$ colour maps with overplotted B band isophotes. *left* Mkn 59; the isophotes correspond to surface brightness levels of 20, 21, 22 and 22.5–25.5 mag/□″ in steps of 0.5 mag. The bright starburst knot (BK), described in detail by Dottori et al. (1994) is indicated. *right* Mkn 71; the isophotes correspond to surface brightness levels of 21, 22, 23, 24, 24.5 and 25 mag/□″. The giant H II complex NGC 2363, as well as the field used to derive the colour–magnitude diagram of the galaxy's underlying stellar population from HST data (CMD 2) are marked. The indices 1–4 along the orientation of the long–slit (centered at the axis origin) mark the regions from which the spectra displayed in Fig. 8 were extracted. North is up and east to the left.

Transformation of dIrrs by RPS should be visible already in a dilute environment, if v_{rel} is sufficiently large. Consequences for their abundances? Star formation?

Metal-Poor cometary BCDs

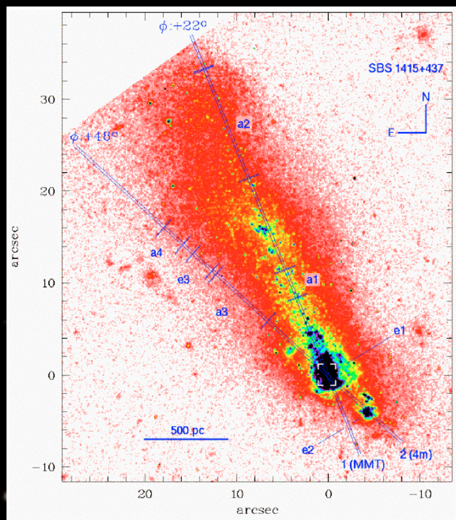

N. G. Guseva et al.: A spectroscopic and p

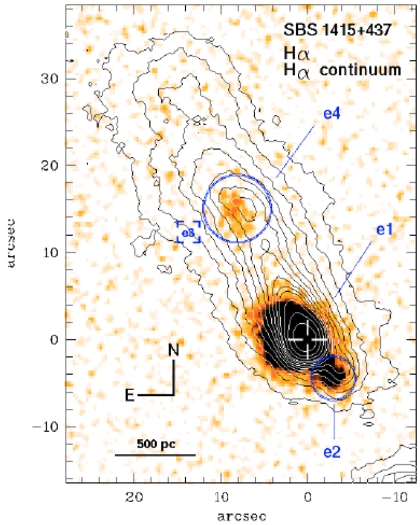

Fig. 2. Continuum-subtracted Hα image of SBS 1415+437 with superposed Hα continuum isophotes. Regions with nebular emission are labeled e1, e2 and e4. The faint region e3 with Hβ and Hα emission lines in its spectrum is not seen in the Hα image.

2017 35

HST V-image of SBS 1415+437.

Guseva et al. (2003, A&A 407, 105)

Questions:

Are Cluster dEs RP stripped dIrrs?

How do transformed dEs look like? Star-formation history, fully gas-evacuated?

DGs are already RP stripped in low-density intergalactic medium! Where to search for them?

Candidates: less frequent than expected! Reasons?

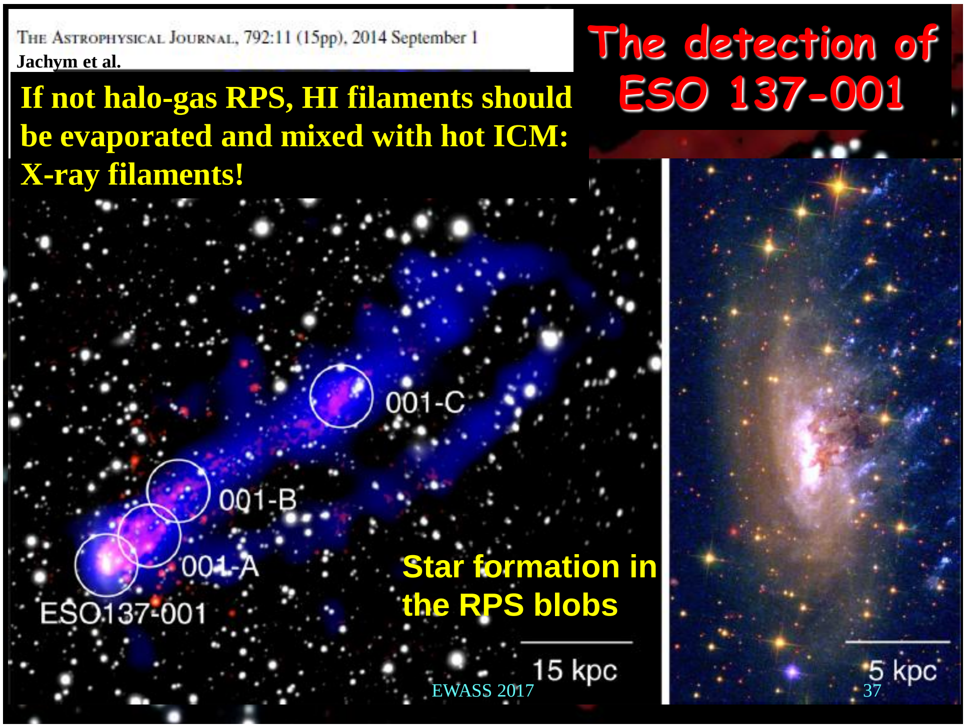
The Astrophysical Journal, 792:11 (15pp), 2014 September 1
Jachym et al.
The detection of ESO 137-001
If not halo-gas RPS, HI filaments should be evaporated and mixed with hot ICM: X-ray filaments!
001-C
001-B
001-A
ESO137-001
Star formation in the RPS blobs
15 kpc
5 kpc
EWASS 2017
37

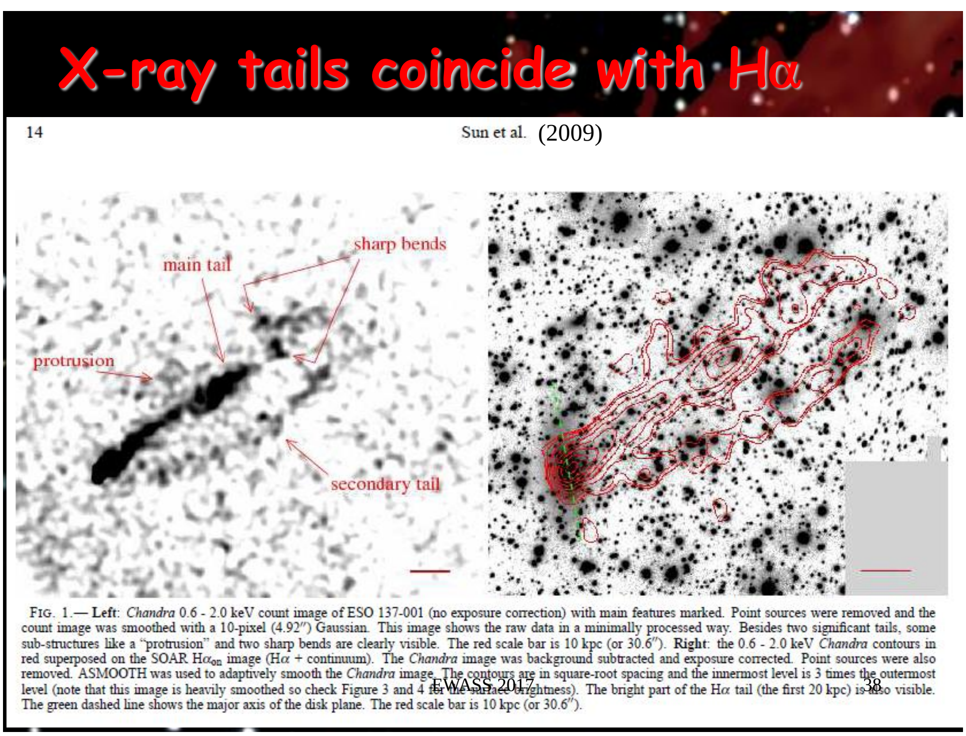
X-ray tails coincide with Hα
14
Sun et al. (2009)
sharp bends
main tail
protrusion
secondary tail
Fig. 1.— Left: Chandra 0.6 - 2.0 keV count image of ESO 137-001 (no exposure correction) with main features marked. Point sources were removed and the count image was smoothed with a 10-pixel (4.92″) Gaussian. This image shows the raw data in a minimally processed way. Besides two significant tails, some sub-structures like a "protrusion" and two sharp bends are clearly visible. The red scale bar is 10 kpc (or 30.6″). Right: the 0.6 - 2.0 keV Chandra contours in red superposed on the SOAR Hα$_{on}$ image (Hα + continuum). The Chandra image was background subtracted and exposure corrected. Point sources were also removed. ASMOOTH was used to adaptively smooth the Chandra image. The contours are in square-root spacing and the innermost level is 3 times the outermost level (note that this image is heavily smoothed so check Figure 3 and 4 for the surface brightness). The bright part of the Hα tail (the first 20 kpc) is also visible. The green dashed line shows the major axis of the disk plane. The red scale bar is 10 kpc (or 30.6″).
EWASS 2017
38

Dwarf Galaxies are expected to lose gas at cluster infall already by the low-density ICM ram pressure

2 *Fumagalli et al.*

How much gas loss? Ram-pressure effects on star formation: In the DG body? In the RPS gas tail?

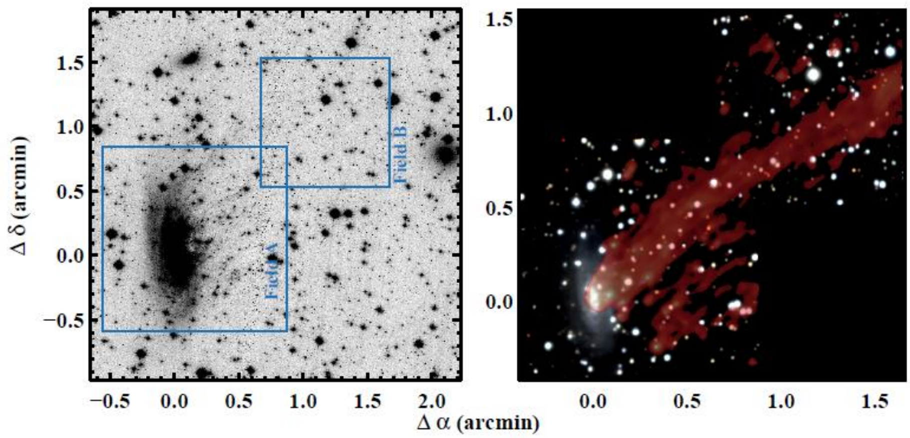

Figure 1. *Left:* Archival HST/ACS image in the F475W filter (PID 11683; PI Ming Sun) with, superposed, the MUSE field of view at the two locations targeted by our observations. In this figure, north is up and east is to the left. The coordinate system is centered at the J2000 position of ESO137−001 (α =16:13:27.3, δ =-60:45:51). *Right:* RGB color image obtained combining images extracted from the MUSE datacube in three wavelength intervals ($\lambda = 5000 - 6000$ Å for the B channel, $\lambda = 6000 - 7000$ Å for the G channel, and $\lambda = 7000 - 8000$ Å for the R channel). A map of the Hα flux is overlaid in red using a logarithmic scale, revealing the extended gas tail that originates from the high-velocity encounter of ESO137−001 with the intracluster medium.

Numerical modeling of RPS DGs

How is gas stripped off from dIrrs?
How does gas react to RP? Clumping, SF enhancement?
How does gas in tails evolve?
Dependence on RP strentgh?

runID	M_g [$M_\odot$]	M_{DM} [10^8 $M_\odot$]	α	v_{rot} [km s^{-1}]	R_{gal} [kpc]	v_{wind} [km s^{-1}]	ρ_{ICM} [g cm^{-3}]
isoHM2	1.4×10^8	8.4	0.9	30.0	9.5	-	-
isoLM2	6.3×10^6	1.2	0.1	2.1	1.3	-	-
rpsLM2	6.3×10^6	1.2	0.1	2.1	1.3	290	10^{-28}
rpsLM3	6.3×10^6	1.2	0.1	2.1	1.3	1000	10^{-27}
rpsLM4	6.3×10^6	1.2	0.1	2.1	1.3	1000	10^{-28}
rpsHM1	1.4×10^8	8.4	0.9	30.0	9.5	290	10^{-28}
rpsHM2	1.4×10^8	8.4	0.9	30.0	9.5	100	10^{-28}

Comparative models of isolated DG evolution

Star-formation self-regulation by stellar feedback

$M_{gas,i}$ = 1.4 x10^8 M$_\odot$; $M_{s,i}$ = 0
M_{DM} = 8.4 x10^8 M$_\odot$
v_{rot} = 30 km/s

- AMR code FLASH

SF as in Köppen, Theis, G.H. (1998, AA, 331)

$\Psi(c,T_c) = C_n c^n \exp\{-T_c/10^4\,K\}$

Low star-formation rate;
No galactic wind!
SF concentr. to the central part;
Structures form; giant gas holes

Steyrleithner & Hensler, in prep.

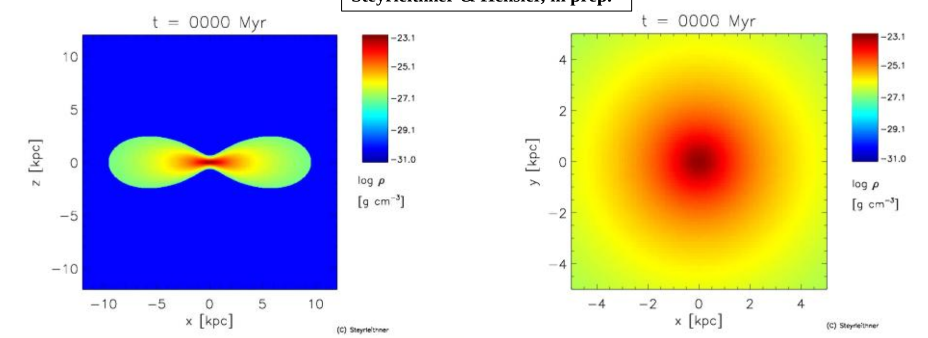

Modelling RPS DGs (HM1)

$M_{gas,i}$ = 1.4 x10^8 M$_\odot$; $M_{s,i}$ = 0
M_{DM} = 8.4 x10^8 M$_\odot$
v_{rot} = 30 km/s
v_{rel} = 290 km/s, n_{ICM} = 10^{-4} cm^{-3}

Steyrleithner & Hensler, in prep.

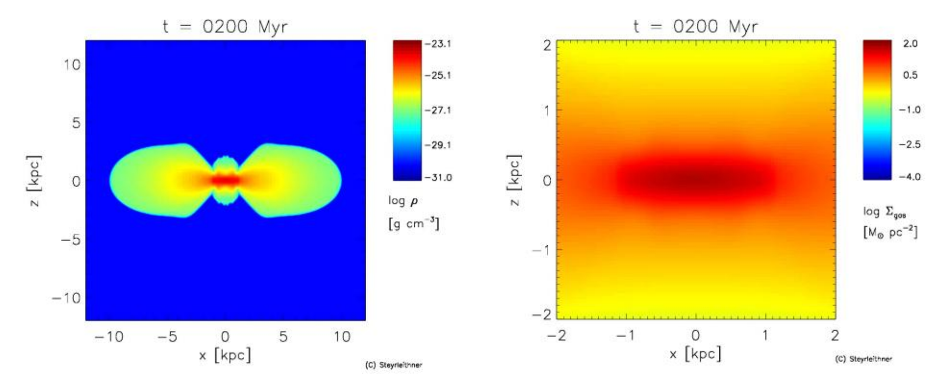

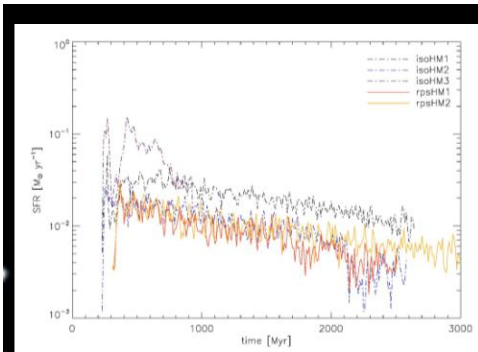

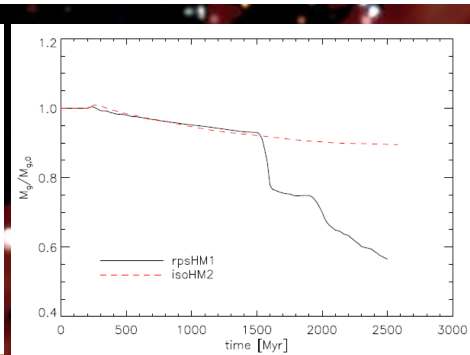

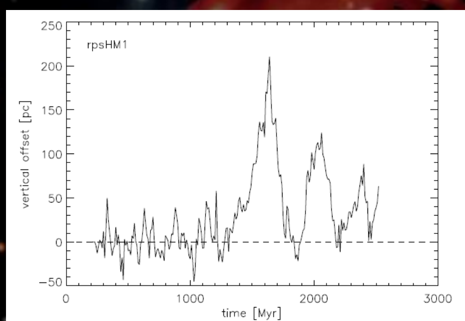

Steyrleithner & Hensler, in prep.

- ✓ No enhanced SF
- ✓ No total gas evacuation
- ✓ Star formation continues at low rate
- ✓ Star-forming sites are dislocated from the disk

RPS for very low-mass DGs (LM1)

$M_{gas,i} = 6.3 \times 10^6\ M_\odot$; $M_{s,i} = 0$
$M_{DM} = 1.2 \times 10^8\ M_\odot$
$v_{rot} = 2$ km/s
moderate infall: $v_{rel} = 290$ km/s,
$n_{ICM} = 10^{-4}\ cm^{-3}$

Steyrleithner & Hensler, in prep.

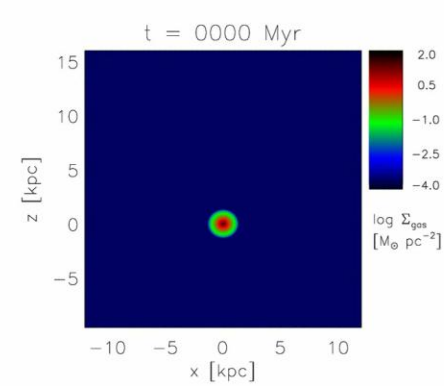

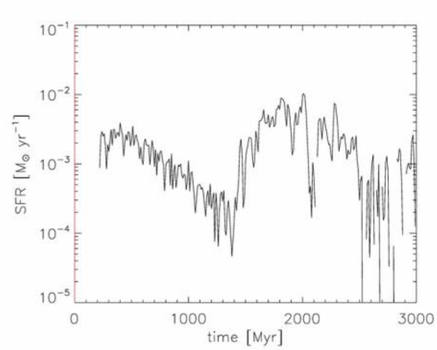

Steyrleithner & Hensler, in prep.

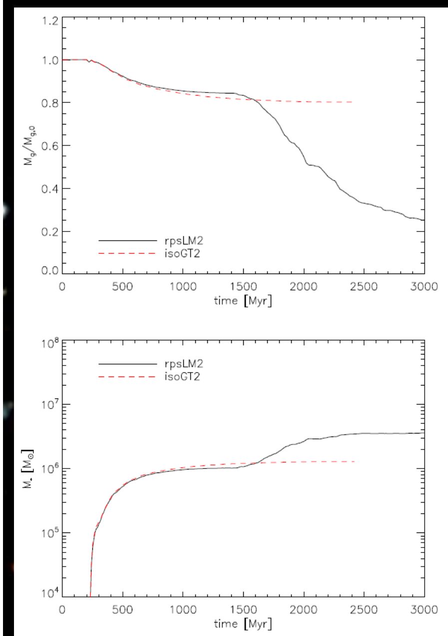

- ✓ SF enhanced by 2 o.o.m. when v_{rel} reaches max.
- ✓ Also max. of RPS mass loss
- ✓ Gas almost totally lost, but condensed clouds survive with varying SFRs
- ✓ Strong oscillating dislocation of SF sites from the plane.
- ✓ No SF in RPS gas tails

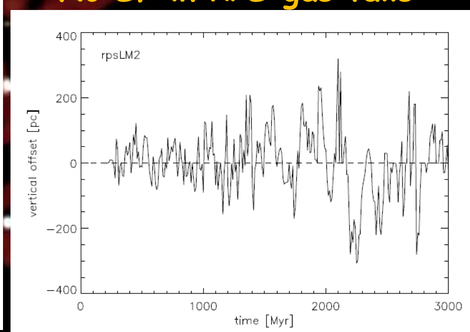

The case of VCC1217

Transformation by RPS

RGB

UV,U,B,V

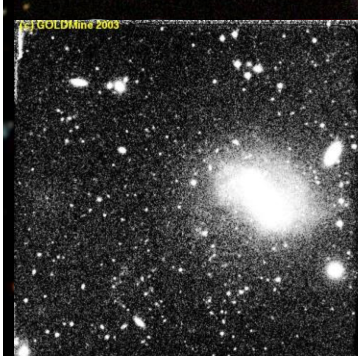

Hα-off

Hα-on
not nec. SF!

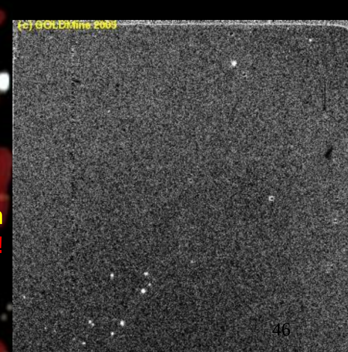

fast RPS DGs (LM4)

$M_{gas,i}$ = 6.3 x10^6 $M_\odot$; $M_{s,i}$ = 0
M_{DM} = 1.2 x10^8 $M_\odot$
v_{rot} = 2 km/s
fast infall: v_{rel} = 1000 km/s,
n_{ICM} = 10^{-4} cm^{-3}

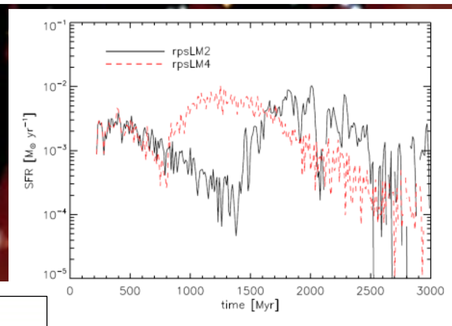

Steyrleithner & Hensler, in prep.

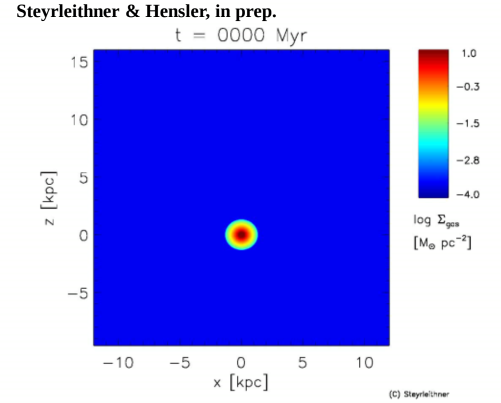

- Critical velocity for enhanced SF is reached earlier not when v_{rel} max.
- Gas almost totally lost, but condensed clouds survive
- When these condensed clumps get RP stipped at later stages, they bear SF.
- A chain of star clusters can be formed from one massive cloud.

2300 Myrs

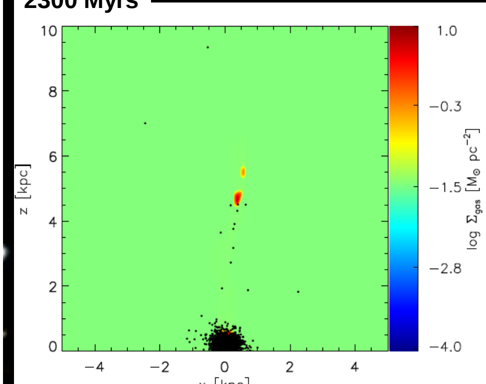

Table 3. Number of formed particles N_{part}, total stellar mass M_*, duration of star burst Δt and the corresponding SFR for the star forming blobs.

Blob	N_{part}	M_* [$M_\odot$]	Δt [Myr]	SFR [$M_\odot$ yr^{-1}]
B3	2	2392	1	2.4×10^{-3}
B4	3	2536	1	2.6×10^{-3}
B4	3	3110	3	1.0×10^{-3}
B4	6	3096	10	3.1×10^{-4}
B4	2	1935	4	4.8×10^{-4}
B4	1	948	1	9.5×10^{-4}
B4	2	2445	1	2.4×10^{-3}
B4	2	1737	1	1.7×10^{-3}
B4	3	1408	3	4.7×10^{-4}

- ✓ Star formation in clumps of various masses.
- ✓ Same cloud experiences multiple SF episodes, chain of star clusters
- ✓ produce several star clusters becoming gas-free: no Hα, purely UV
- ✓ Local oscillations of SF sites produce dE shape and vel. dispersion.

But:

- ✓ Very low SFRs: IMF not filled! Consequences for SFR determination!
- ✓ Physical processes taken into account.

Study RPS and star formation in high-velocity clouds

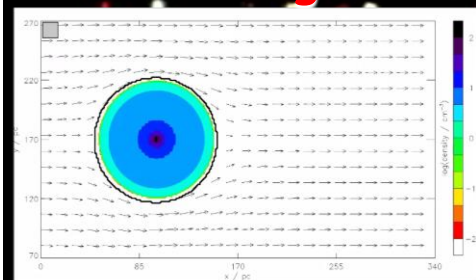

Sander & Hensler, in prep.

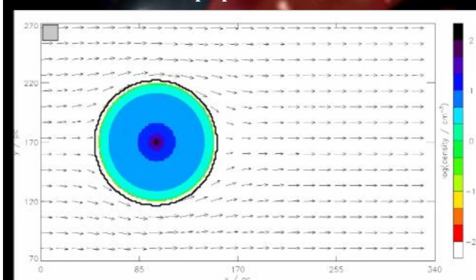

M_{cl} = 8.75 x10^4 $M_\odot$ no M_{DM}
R_{cl} = 48.42 pc
n_{ICM} = 7 x 10^{-4} cm^{-3}

slow infall: v_{rel} = 167 km/s, Ma=0.4

fast infall: v_{rel} = 333 km/s, Ma=0.9

Only high v_{rel} leads (due to compression) gravitationally bound clouds to Jeans instab. and sf.

Conclusions on cluster DGs RPS

dEs in clusters are

- distinguishible between those born in the cluster and those fallen in (and passing through), respectively, within the last Gyrs; e.g. bluich cores.
- RPS of infalling dIrrs occurs in cluster outskirts already
- at low ram pressure,
- at large relative velocities compression leads to Jeans instability and star formation;
- Multiple gas-free clusters are formed (some chain like)
- dE shape by enhanced stellar vel. dispersion

Stellar content, MAss and Kinematics of Cluster Early-type Dwarfs (SMAKCED): project of dEs in Virgo Cl.

http://www.smakced.net

Urich, L., Lisker, T., Janz, J., et al. (HENSLER, G.):
Young, metal-enriched cores in early-type dwarf galaxies in the Virgo cluster based on colour gradients,
2017, Astron. Astrophys., submitted

Sen, S., Peletier, R.F., Boselli, A., et al. (HENSLER, G.):
Na and Ca abundances in dwarf elliptical galaxies, 2017, MNRAS, submitted

Toloba, E., Guhathakurta, P., Boselli, A., et al. (HENSLER, G.):
Stellar Kinematics and structural Properties of Virgo Cluster Dwarf early-type Galaxies from the SMAKCED Project. III. Trends as a Function of projected Distance from the Cluster Center. 2015, ApJ., 799, 172

Toloba, E., Guhathakurta, P., Peletier, R.F., et al. (HENSLER, G.):
Stellar Kinematics and structural Properties of Virgo Cluster Dwarf early-type Galaxies from the SMAKCED Project. II. The Survey and a systematic Analysis of kinematic Anomalies and Asymmetries..
2014, ApJ. Suppl., 215, 17

Janz, J., Laurikainen,, E.,Lisker, T., et al. (HENSLER, G.):
A Near-Infrared Census of the Multi-Component Stellar Structure of Early-Type Dwarf Galaxies in the Virgo Cluster . 2014, ApJ, 786, 105

Toloba, E., Guhathakurta, P., van de Ven, G., et al. (HENSLER, G.):
Stellar Kinematics and Structural Properties of Virgo Cluster Dwarf Early-Type Galaxies from the SMAKCED Project. I. Kinematically Decoupled Cores and Implications for Infallen Groups in Clusters . 2014, ApJ, 783, 120

Janz, J. Laurikainen, E. Lisker, T., et al. (HENSLER, G.):
Dissecting early-type dwarf galaxies into their multiple components . 2012, ApJL, 745, L24